disturbance affected the observations, which could, if understood, possibly be included in the functional model for the tidal analysis.

Acknowledgements: We thank H.-G. Wenzel for the ETERNA source code and discussions, G. Polzer for help with the fits for the NDFW parameters and the "Deutsche Forschungsgemeinschaft" for financial support (We 1653/1).

References

Blackman, R. B., Tukey, J. W., 1958. The measurement of power spectra. Dover Publ., New York, 190 pp.

Friederich, W., Wilhelm, H. 1986. Solar Radiational Effects on Earth Tide Measurements. In: *Proc. 10th Int. Symp. Earth Tides* (R. Vieira, Ed.), Cons. Sup. Invest. Cient., Madrid, pp. 865 - 880.

Hinderer, J. 1997. Constraints on the Earth's Deep Structure and Dynamics from Superconducting Gravimetry. In: Earth's Deep Interior (Ed. D. J. Crossley), Chapt. 6, Gordon and Breach Sci. Publ., Amsterdam, 167 - 195.

Lindberg, C. R., Park, J. J. 1987. Multiple-taper spectral analysis of terrestrial free oscillations, Part 2. *Geophys. J. R. astr. Soc.* **91**: 795 - 836.

Merriam, J. 1994. The Free Core Nutation Resonance in Gravity. *Geophys. J. Int.* **119**: 369 - 380.

Park, J., Lindberg, C. R., Thomson, D. J. 1987. Multiple-taper spectral analysis of terrestrial free oscillations, Part 1. *Geophys. J. R. astr. Soc.* **91**: 755 - 794

Polzer, G., Zürn, W., Wenzel, H.-G. 1996. NDFW Analysis of Gravity, Strain and Tilt Data from BFO. *Bull. Inf. Marées Terrestres* **125**: 9514 - 9545.

Riede, M. 1997. Gezeitenanalyse bei nicht-stationären Störsignalen: Einflüsse verschiedener Datenfenster. Diploma Thesis, Faculty of Physics, Karlsruhe University, 87 pp.

Tamura, Y. 1987. A harmonic development of the tide-generating potential. *Bull. Inf. Marées Terrestres* **99**: 6813 - 6855.

Wenzel, H.-G. 1994. Earth tide analysis package ETERNA 3.2. *Bull. Inf. Marées Terrestres* **118**: 8719 - 8721.

Wenzel, H.-G. 1997. Analysis of Earth Tide Observations. In: Tidal Phenomena (H. Wilhelm, W. Zürn and H.-G. Wenzel, Eds.), *Lecture Notes in Earth Sciences* **66**, Springer, Heidelberg, 59 - 75.

Widmer, R., Zürn, W., Masters, T. G. 1992. Observation of low order toroidal modes from the 1989 Macquarie Rise event. *Geophys. J. Int.* **111**: 226 - 236.

Zürn, W. 1997. The Nearly-Diurnal Free Wobble-Resonance. In: Tidal Phenomena (H. Wilhelm, W. Zürn and H.-G. Wenzel, Eds.), *Lecture Notes in Earth Sciences* **66**, Springer, Heidelberg, 95 - 109

1998

Proper Usage of the ICET Data Bank
Du bon usage de la Banque de Données ICET

Comparison with theoretical applications on Earth Models

P. Melchior and O. Francis

Observatoire Royal de Belgique
Avenue Circulaire, 3
B-1180 Brussels
Belgium
E-mail: melchior@oma.be, francis@oma.be

1. Introduction

The information contained in the ICET Data Bank DB92 has to be used with caution and on the basis of a critical selection depending upon the objectives of investigations as stated by Melchior (1994, alinea 12):

(1) historical data, see for example the discussion of Tomaschek measurements by Melchior (1995 b) and by Wenzel (1995);

(2) systematic behaviour of some instruments used in profiles in order to improve the homogeneity and consistency of the Data Bank, see for example Baker et al. (1996);

(3) data from stations affected by large oceanic effects used to check and compare oceanic tides models, see for example Melchior and Francis (1996);

(4) data from stations where the oceanic effects are small (proportionally to the body tide) or well controlled (10% uncertainty or less on L vector amplitude) to test Earth's body tide models for the tidal waves O_1, K_1, P_1 and M_2 including the possibility of lateral heterogeneity effects.

Misapplications of these criteria, in the past, sometimes led to misclaims or misunderstanding. The last two criteria correspond to the objective of the present paper.

2. Comparisons with Earth's body tide models for the two main lunar waves O_1 and M_2

For such comparisons we have selected:

(a) European continental stations at mid-latitudes (where M_2 and O_1 waves have practically equal amplitudes around 35µgal), i.e. 20 series selected in function of the high quality of their instrumentation (Table 1 for the M_2 wave ; Table 3 for the O_1 wave);

(b) the important network covering the large South American continent which includes 34 stations, where the M_2 amplitude reaches up to 80 µgal but where the diurnal waves amplitudes are small (Table 2, excluding Central America and Patagonian shelf).

It is worth while to point out that all small islands were excluded as well as Indonesia, Philippines and Japan. Australian and New Zealand stations had to be excluded because of the poor quality of the oceanic models in this area (Melchior and Francis, 1996). Chinese network was not considered because data were made available to ICET only for the ten stations occupied by the Royal Observatory of Belgium. Data from North America are too few. We do not use here the results obtained in Africa as there is a real suspicion of lateral heterogeneity effects between the cold spot in the Western part and the hot spot in the horn of Africa (Melchior 1995a).
We have also rejected all stations exhibiting, after ocean tide loading corrections, phase lags (or advances) larger than 0.5° on O_1 or M_2 as well as large X residues $|X| > |B|$, (instrumental phase lag determination being sometimes doubtful). A well identified critical point is the accuracy of the instrumental calibrations. A criterion about it may be that if the results for the O_1 wave are coherent with the models, the results for the M_2 wave are not biased by calibration effects even if they exhibit anomalies.

2.1. Wave M_2

The M_2 oceanic loading corrections in Western and Central Europe are of the order of 1 to 2 µgal, that is about 6% of the observed amplitude. However, they reach twice (or even more) this amplitude in Spain (Francis and Melchior, 1996). From the Tables 1 and 2, it comes out that the inelastic non-hydrostatic Earth body model (α = 0.15) results (Dehant et al. 1997) 1.16257 is close to and comprised between the experimental solutions based upon CSR3.0 and FES95.2 oceanic models in Europe and in South America involving 52 tidal gravity stations and 26 different gravimeters:

	Europe	South America
FES95.2	1.1604 ± 0.0003	1.1603 ± 0.0012
CSR3.0	1.1633 ± 0.0007	1.1607 ± 0.0012

The standard 1980 Schwiderski model gives a 0.2% lower δ factor (δ = 1.1580). With all models and in both continents the phase is negative, around -0.05° in Europe but around -0.30° in South America.
Considering the higher quality of the instruments used and the optimum installation conditions in Observatories in Europe (superconducting gravimeters and LaCoste Romberg Earth Tide meters) we should mainly thrust the smallest phase lag. However the South America results fit almost exactly the value obtained by regression calculations between the **B** and **L** vectors obtained from 300 stations of DB92, i.e. -0.3° (Melchior 1989 and alinea 4 of the present paper). At most (50) of the continental European stations, including Scandinavia the CSR3.0 results are 1% higher than SCHW80 while FES95.2 results are 0.5% higher. There is thus a difference of 0.5% between CSR3.0 and FES95.2 results. For the twenty stations in Spain these differences with respect to SCHW80 are 0.5% higher for CSR3.0 and practically 0 for FES95.2 thus still 0.5% between CSR3.0 and FES95.2.

2.2. Wave O_1

The oceanic contribution in tidal gravity is rather small in Europe for the O_1 wave. As an example, the oceanic tides at Oostend harbour in Belgium have an amplitude of only 0.095 m for O_1 against 1.803 m for M_2.

Thus the corrections on the O_1 amplitude are of the order of 0.15 microgal (i.e. 0.4% of th observed O_1 amplitude) with only slight differences between the oceanic models.
On the basis of the 20 European series selected (Table 3), the δ factor differs only at the fourtl decimal, depending on the oceanic model used for the correction for loading:

$$\delta(O_1) = 1.1531 \text{ to } 1.1538 \ (\pm 0.0005)$$

in fair agreement with the anelastic, non-hydrostatic model of Dehant et al. (1997) 1.15382 the phase lag being:

$$\alpha(O_1) = -0.01° \text{ to } -0.07° \ (\pm 0.01°)$$

3. The Diurnal Tidal Gravity Waves and the Earth's Liquid Core Resonance

Obviously, it is of great interest to examine the four important diurnal waves Q_1, O_1, P_1 and K_1 in view of a comparison with the Earth liquid core resonance as given by the recent theoretical models. However not many stations can be used for this purpose because series longer than 180 days are needed to perform a separation of the waves P_1 and K_1 from the spurious S_1 meteorological component. Moreover equatorial and sub-tropical stations are not suitable because the amplitude of all tesseral diurnal waves vanishes at the equator. We therefore selected the convenient series according to the following criteria:
1.- Length of continuous measurements : more than 180 days.
2.- Latitude higher than + 23° (Northern hemisphere) or - 23° (Southern hemisphere) : the observed P_1 amplitude varies from 12 µgal at the tropic (Alice Springs station) to 17 µgal at the latitude 45° (Ottawa station).
3.- Instrumental calibration accuracy checked.
4.- Mean square error on the P_1 phase ($E(\alpha P_1)$) less than 0.3°.
5.- Oceanic loading amplitude ratio to observed amplitude (B/A) < 0.05

Twenty seven stations with thirty two different gravimeters satisfying these five criteria are listed in Table 4 where not only the δ, α parameters corrected for oceanic effects (Schwiderski models) but also the B, L and X vectors are given. Despite their small amplitudes the B and L vectors remarkably fit together so that, in practically all cases, the X amplitudes are reduced with respect to the B amplitudes. For these 27 stations (amongst which 12 outside Europe) vectorial means are to be compared with the inelastic non-hydrostatic model of Dehant et al. (1997):

Wave	27 World Stations		15 European stations		Model*
	δ	α	δ	α	δ
Q_1			1.1524±0.0006	-0.06°±0.03°	1.1538
O_1	1.1556±0.0008	-0.12°±0.04°	1.1538±0.0006	0.00°±0.02°	1.1538
P_1	1.1485±0.0009	-0.01°±0.05°	1.1477±0.0007	0.02° ± 0.03°	1.1487
K_1	1.1379±0.0008	- 0.05°±0.04°	1.1356±0.0007	0.06°±0.02°	1.1345

* Dehant, Defraigne and Wahr (1997).
δ, α tidal parameters corrected for oceanic loading

For Q_1 we have restricted the selection to those stations where $|\alpha \text{ corrected}| < 0.4°$ and L (Q_1) < 0.10 µgal. 17 European series satisfying these conditions are given in Table 5. The differences in the oceanic loading corrections according to the different O_1 oceanic models are negligible for stations distant by more than 100 km from the shore, as shown by Melchior and Francis (1996 - equation (3)). This applies also to Q_1, P_1 and K_1 waves.

4. Residues obtained for the different tidal constituents:

We use the notations introduced in all our previous papers (Melchior, 1983, page 389). Melchior and Francis (1996) recently analysed in details all the data of the ICET Data Bank (DB 92) obtained for the main lunar waves O_1 and M_2 and concluded that regressions and correlation coefficients k between the B and L vectors gave, for 11 different oceanic tide models, the following World means:

	M_2	O_1
In phase component		
a_c	-0.034 ± 0.057	-0.120 ± 0.027
b_c	1.125 (48.4°) ± 0.019	0.988 (44.6°) ± 0.039
k_c	0.874 to 0.930	0.825 to 0.835
Out of phase component		
a_s	-0.273 ± 0.065	-0.015 ± 0.023
b_s	1.094 (47.6°) ± 0.011	0.919 (42.6°) ± 0.036
k_s	0.919 to 0.941	0.791 to 0.840

We will consider here the other main tidal waves: Q_1, P_1, K_1 and N_2, as oceanic corange-cotidal models are also available for these more or less important constituents. However a comparison with any ground based tidal gravity station is not obvious.

4.1 Lunar Waves

Besides the purely lunar waves of largest amplitude, the tesseral diurnal component O_1 and the sectorial semi-diurnal component M_2, the luni-solar tidal potential development contains two important lunar waves generated by the ellipticity of the lunar orbit (eccentricity 0.0549): the "elliptic" companion of O_1, called Q_1, and the "elliptic" companion of M_2, called N_2, whose amplitudes are both in the ratio 0.1915 of their "mother" wave. Their frequencies also differ by the same amount (0.544°/hour, that is 360° in a mean anomalistic month) from their "mother" wave frequency.
The waves Q_1 and N_2 can thus be considered just as O_1 and M_2 as one anomalistic month data allows a correct determination but they have, in general, a small amplitude with respect to the instrumental noise. Thus a quite longer series of measurements is needed. With periods of 26.868 hours and 12.658 hours these two waves are practically not disturbed by the atmospheric pressure effects which are concentrated around 24 hours and 12 hours. At 45° latitude they are of comparable amplitudes (respectively 5.95 and 7.19 µgal for a rigid Earth) and have exactly equal amplitude at 50.38° latitude.

4.1.1. The diurnal lunar wave Q_1

The diurnal waves are resonant only in few restricted oceanic areas: Aden, East Asia, North Pacific, South Australia, Patagonia, Carribean and Antarctic. It results that the amplitudes of the vectors **B** (Q_1) and **L** (Q_1) remain less than 0.1 µgal in all other areas, particularly in Europe and West Africa.
An amplitude of one microgal has been observed for B at only one station, Comandante Ferraz in the South Shetlands where we get :

$B = 1.25$ µgal, $\beta = -163°$ $\quad L = 0.92$ µgal , $\lambda = -159°$ (FES95.2) $X = 0.34$ µgal, $\chi = -174°$

With 223 stations from the DB92 Data Bank (several stations exhibiting obvious large anomalies being discarded) we obtain as correlation coefficients: $k_c = 0.747$, $k_s = 0.754$. The Table 6 shows that, for what concerns these correlation coefficients the four models SCHW80, CSR3.0, FES95.2 and ORINAO do not differ significantly. Also the independent terms a_c, a_s in the regression do not differ significantly while they are small and negative in all cases which again could correspond to a small phase lag of the Earth's body tide. The regression coefficients b_c, b_s exhibit more discrepancies and the CSR3.0 model obviously looks more satisfactory than the others. However, the observed load is slightly larger than the calculated one:

$b_c = 1.133 \pm 0.067$ (48.6°) $\qquad b_s = 1.028 \pm 0.059$ (45.8°)

In many of these 223 stations, the L amplitudes are very small, even vanishing, while the corresponding very small B amplitudes are often overwhelmed by local noise which makes the correlation illusory.
Considering that the standard error on the observed amplitudes B is about 0.2 µgal, we have selected those ground based tidal gravity stations where L (Q_1) ≥ 0.20 µgal, a situation which arises essentially around the Indian, Pacific and Antarctic Oceans as well as in some South American Coastal stations. Thirty-three stations fulfilling this criterion are reported in Table 7. These stations obviously are not the same as those listed in the Table 5 which were selected on the basis of the opposite criterion i.e. L (Q_1) ≤ 0.05 µgal. The stations of Table 7 are not suitable for testing the Earth's body tidal models.
To calculate the regression between the in-phase and out-of-phase components of vectors **B** and **L** we have added three European stations equipped with superconducting gravimeters. This has given for the 36 stations:

Wave Q_1 (36 stations) where L (Q_1) ≥ 0.20 µgal

Parameters	SCHW80	CSR3.0	FES95.2
In-phase component			
a_c	-0.046±0.018	- 0.052 ± 0.015	- 0.015 ± 0.017
b_c	1.260 (51.6°)±0.062	1.105 (47.9°) ± 0.045	1.261 (51.6°) ± 0.057
k_c	0.961	0.972	0.966
RMS	0.106	0.090	0.099
Out-of-phase component			
a_s	- 0.032 ± 0.025	- 0.014 ± 0.028	- 0.057 ± 0.025
b_s	1.206 (50.3°) ± 0.114	0.801 (38.7°) ± 0.089	1.068 (46.9°) ± 0.105
k_s	0.873	0.836	0.865
RMS	0.143	0.161	0.147

4.1.2. The semi-diurnal wave N_2

The oceanic loading effects are evidently larger than those of the diurnal wave Q_1, due to the resonances observed in the world oceans at semi-diurnal frequencies. For the N_2 wave they are however still very small in Scandinavia, West Africa and China, still rather small in Western Europe (around 0.35 µgal) but reach 1 µgal or more in Spain. They are of the microgal level in East and South Africa and South America (with the exception of Argentina). A correlation analysis applied to 206 stations of the data bank, where L (N_2) ≥ 0.20 µgal, has given :

Wave N_2 (206 stations) where L (N_2) ≥ 0.20 µgal

Parameters	SCHW80	CSR3.0	FES95.2
In-phase component			
a_c	- 0.024 ± 0.016	0.034 ± 0.016	0.030 ± 0.016
b_c	0.991 (44.7°) ± 0.030	0.908 (42.2°) ± 0.030	1.014 (45.4°) ± 0.030
k_c	0.917	0.911	0.926
RMS	0.224	0.231	0.212
Out-of-phase component			
a_s	- 0.034 ± 0.020	- 0.037 ± 0.019	- 0.058 ± 0.019
b_s	1.000 (45°) ± 0.032	0.968 (44.1°) ± 0.028	1.065 (46.8°) ± 0.032
k_s	0.911	0.923	0.921
RMS	0.236	0.220	0.223

4.2. Solar and luni solar waves

We do not consider here S_2 and K_2 waves because atmospheric pressure corrections are not available for most of the stations. Moreover the admittance coefficient (µgal/mbar) is different in function of the geographical and climatic conditions, coastal or continental situation. The P_1 and K_1 constituents have large amplitudes but they are close in frequency so that long series of data (six months or, better, one year) are needed to separate P_1 from K_1. Moreover these two waves are influenced by the atmospheric effects. Series of one year length, with atmospheric pressure data, would thus be needed to correctly determine their parameters. In general the ocean is not resonant at their frequencies and, consequently, do not generate strong attraction and loading effects. Very few stations exhibit significant P_1 and K_1 residues.

4.2.1. The diurnal solar wave P_1

The situation is similar to the Q_1 wave: only those areas where the ocean tidal diurnal frequencies give measurable residues. But here, the length of the series of observations must be at least six months and the observing room must be well protected against temperature variations. We thus have considered again here only those stations where L (P_1) ≥ 0.20 µgal that is stations which are not suitable for testing the Earth's body tidal models and, consequently, differ from those listed in Table 4 which obey to the opposite criterion L (P_1) ≤ 0.10 µgal (the maximum P_1 body tide amplitude being 16.7 µgal at the latitude 45°). We found only 26 series in the Data Bank DB92 which fulfil these three conditions (Table 8). The **L** vectors are comprised between 0.2 and 1 microgal and the differences between the oceanic models considered here (SCHW80, CSR3.0 and FES95.2) are in general well below the observations noise. The regression calculations give the following results:

Wave P_1 (27 stations) where L (P_1) ≥ 0.20 µgal

Parameters	SCHW80	CSR3.0	FES95.2
In-phase component			
a_c	0.040 ± 0.047	0.056 ± 0.045	0.037± 0.047
b_c	1.170 (49.5°) ± 0.088	0.998 (44.9°) ± 0.072	1.057 (46.6°) ± 0.080
k_c	0.934	0.939	0.932
RMS	0.241	0.233	0.244

Out-of-phase component

a_s	- 0.016 ± 0.026	- 0.019 ± 0.029	- 0.002 ± 0.031
b_s	1.088 (47.4°) ± 0.063	0.837 (39.9°) ± 0.054	0.878 (41.3°) ± 0.062
k_s	0.959	0.950	0.941
RMS	0.137	0.151	0.163

4.2.2. The diurnal luni-solar wave K_1

Considering that the problems of extraction of the wave K_1 are exactly the same of those o the wave P_1, we have, for reasons of homogeneity, selected the same 26 stations used for th wave P_1 as listed in the Table 9. One may remind here that the K_1 amplitude is three times th P_1 amplitude in the development of the luni-solar potential. In the oceans this ratio is slightly higher, being 3.3, due to the small difference in the frequencies (0.082°/hour) while the λ phases differ in general by no more than 2° from those of P_1. Thus to L (P_1) ≥ 0.2 µga corresponds L (K_1) ≥ 0.6 µgal.
It may be interesting to point out that, for two equatorial stations in Table 9, Mogadiscio and Quito, the B or L amplitudes are respectively larger and equal to the observed A amplitude which had to be expected as the Earth's body tide vanishes at the equator.

Wave K_1 (27 stations) where L (P_1) ≥ 0.20 µgal

Parameters	SCHW80	CSR3.0	FES95.2
In-phase component			
a_c	- 0.099 ± 0.106	0.067 ± 0.108	0.012 ± 0.93
b_c	1.220 (50.6°) ± 0.64	1.072 (47°) ± 0.58	1.168 (49.4°) ± 0.54
k_c	0.967	0.965	0.975
RMS	0.535	0.551	0.471
Out-of-phase component			
a_s	- 0.179 ± 0.112	- 0.163 ± 0.105	- 0.134 ± 0.110
b_s	0.919 (42.6°) ± 0.084	0.746 (36.7°) ± 0.064	0.801 (38.7°) ± 0.072
k_s	0.909	0.920	0.913
RMS	0.570	0.537	0.560

5. The problem of the phase lag

The problem of the Earth tides phase lag has long been a source of contests and contradictions. It is however a crucial parameter for the budget of Earth's rotation secular retardation and moon acceleration.
For the main wave M_2, directly responsible for the secular retardation of the Earth's rotation, the instruments of high quality installed in observatories offering the best conditions, all situated in Europe, give (Table 1) for these α_g phase related to the gravimetric disturbance at the deforming surface (Zschau 1978) and corresponding to the (h - 3/2 k) combination of the Love numbers:

phase α_g	oceanic model corrections according to
- 0.07° ± 0.03°	SCHW80
- 0.12° ± 0.03°	CSR3.0
0.00° ± 0.03°	FES95.2
- 0.07° ± 0.03°	FES95.2b

However 34 stations in South America, involving 10 different instruments give very homogeneous phase lags for the same four oceanic models (Table 3):

$$\alpha = - 0.30° \pm 0.06°$$

We should trust the null or small phase lags obtained in Europe but an explanation is then needed for the South American continent.

The linear regressions calculated between the cosine and sine components of the **B** and **L** vectors give for all waves and with each one of the 11 oceanic tides models (see Melchior and Francis 1996, Table 2) systematic negative values, through not always significant for the independent terms a_s (M_2, N_2, O_1, Q_1, P_1, K_1) and a_c (same waves at the exception of N_2 and P_1).

$$a_s \cong - 0.273 \pm 0.060$$

This could be explained by a phase lag of about -0.3° corresponding to a pressure effect **P** as advocated by Schwiderski (1985) or Platzmann (1985). The vectorial representation of the residues should thus be written

$$\mathbf{B}^* = \mathbf{A} - (\mathbf{R} + \mathbf{P}), \qquad \mathbf{X}^* = \mathbf{B}^* - \mathbf{L} = \mathbf{B} - \mathbf{L} - \mathbf{P}$$

If **P** is in quadrature with **R** one gets

$$X^* \cos\chi^* = X \cos\chi, \qquad X^* \sin\chi^* = X \sin\chi - P$$

Then, taking $P \cong X \sin\chi = - 0.154 \pm 0.028$ µgal, reduces the phase lag α_g to zero.

Using VLBI measurements, Mitrovica et al. (1994) determined the h_2 Love number and phase characterising the radial displacement in the tesseral diurnal part of the tidal potential. They obtained for the O_1 lunar wave:

$$h_2(O_1) = 0.614 \pm 0.007, \qquad \alpha_r(O_1) = - 0.7° \pm 0.5°$$

a phase which is the tidal bulge delay angle of the Earth's radial displacement, different from the "gravimetric bulge" α_g which is related to the (h_2 - 3/2 k_2) combination of Love numbers (Zschau, 1978).

A direct measurement of this bulge delay angle α_r can also be obtained from registration of the radial deformations with a vertical extensometer. To our knowledge only one such instrument has given significant results, a 3.4 meter long quartz tube fixed in the ceiling of a mine gallery in the Walferdange Underground Laboratory. At Walferdange latitude (49.665° N) the theoretical amplitude of the radial component of the M_2 deformation tensor:

$$e_{rr} = [- \upsilon/(1 - \upsilon)] (2h - 6 l) W_2/ag \qquad \text{(Melchior 1983, section 3.3.5)}$$

(with υ: Poisson coefficient) is

$$R = 11.244\ 10^{-9}, \text{ zero phase}$$

when we take for reference model the physical limit of an incompressible elastic Earth

$$\upsilon = 0.5 \text{ with } h = 0.62,\ l = 0.09$$

The oceanic perturbation in the radial extension, calculated on the basis of the Schwiderski M_2 model is

$$L = 0.682\ 10^{-9} \qquad \lambda = - 118.85°$$

We have

$$A_0 = R + L = 11.57\ 10^{-9} \qquad \alpha_0 = + 2.95°$$

while the analysis of two long series of registration of the vertical extensometer (1971-78 and 1980-83) gives

$$A = 7.613\ 10^{-9} \qquad \alpha = + 2.54° \pm 0.23°$$

Thus a phase lag

$$\alpha_r = \alpha - \alpha_0 = - 0.41° (\pm 0.23°)$$

(Note that a change of the elastic reference model do not affect the phases).

It may be interesting to point out that the observed phase lag of the tidal gravity (vertical component) obtained with three Askania gravimeters installed very close to this extensometer

is $\alpha = 2.17° \pm 0.01°$ and, corrected for oceanic effects : $\alpha_g = - 0.32°$ ($\pm 0.01°$) coincidence or true geophysical fact?

Bibliography

Baker, T.F., Curtis, D.J. and Dodson, A.H,.1996. A new test of Earth tide models in central Europe, Geophys. Res. Letters 23, 3559-3562.

Dehant, V, Defraigne, P. and Wahr, J-M.,1997. Tides for a convective Earth, 13th Symposium on Earth Tides. Bruxelles 1997, this volume.

Francis O. and Melchior P., 1996. Tidal loading in South Western Europe: A test area, Geophysical Research Letters, 23, 2251-2254.

Melchior, P., 1983. The tides of the planet Earth. Oxford: Pergamon Press.

Melchior, P., 1989. The phase lag of Earth tides and the braking of the earth's rotation, Phys. Earth Planet Int., 56: 186-188.

Melchior, P., 1994. A new data bank for tidal gravity measurements (DB92), Phys. Earth Planet Int., 82: 125-155.

Melchior, P., 1995a. A continuing discussion about the correlation of tidal gravity anomalies and heat flow densities, Phys. Earth Planet Int., 88: 223-256.

Melchior, P., 1995b. About Data Rescue . An historical tidal gravity series of R. Tomaschek, Bull. Inf. Marées Terrestres 123, 9365-9366.

Melchior, P. and Francis, O., 1996. Comparison of Recent Ocean Tide Models Using Ground-Based Tidal Gravity Measurements, Marine Geodesy, 19, 291-330.

Mitrovica, J.X., Davis, J.L., Mathews, P.M. and Shapiro, I.I., 1994. Determination of tidal h Love number parameters in the diurnal band using an extensive VLBI data set, Geophys. Res. Letters, 21: 705-708.

Platzmann, G.W., 1985. The Role of Earth Tides in the Balance of Tidal Energy, J. Geophys. Res. 90: 1789-1793.

Schwiderski, E., 1985. On tidal friction and the deceleration of the Earth's rotation and Moon's revolution, Marine Geodesy, 9: 399-450.

Wenzel, H-G.,1995. Re-analysis of Tomaschek's gravity tide observations made in 1954 at Baltasound, Shetland Islands, Bull. Inf. Marées Terrestres, 123, 9367-9373.

Zschau, J., 1978. Tidal Friction in the Solid Earth Loading Tides Versus Body Tides, in Tidal Friction and the Earth's Rotations, edited by P. Brosche and J. Sündermann. Springer-Verlag Berlin pp 62-94.

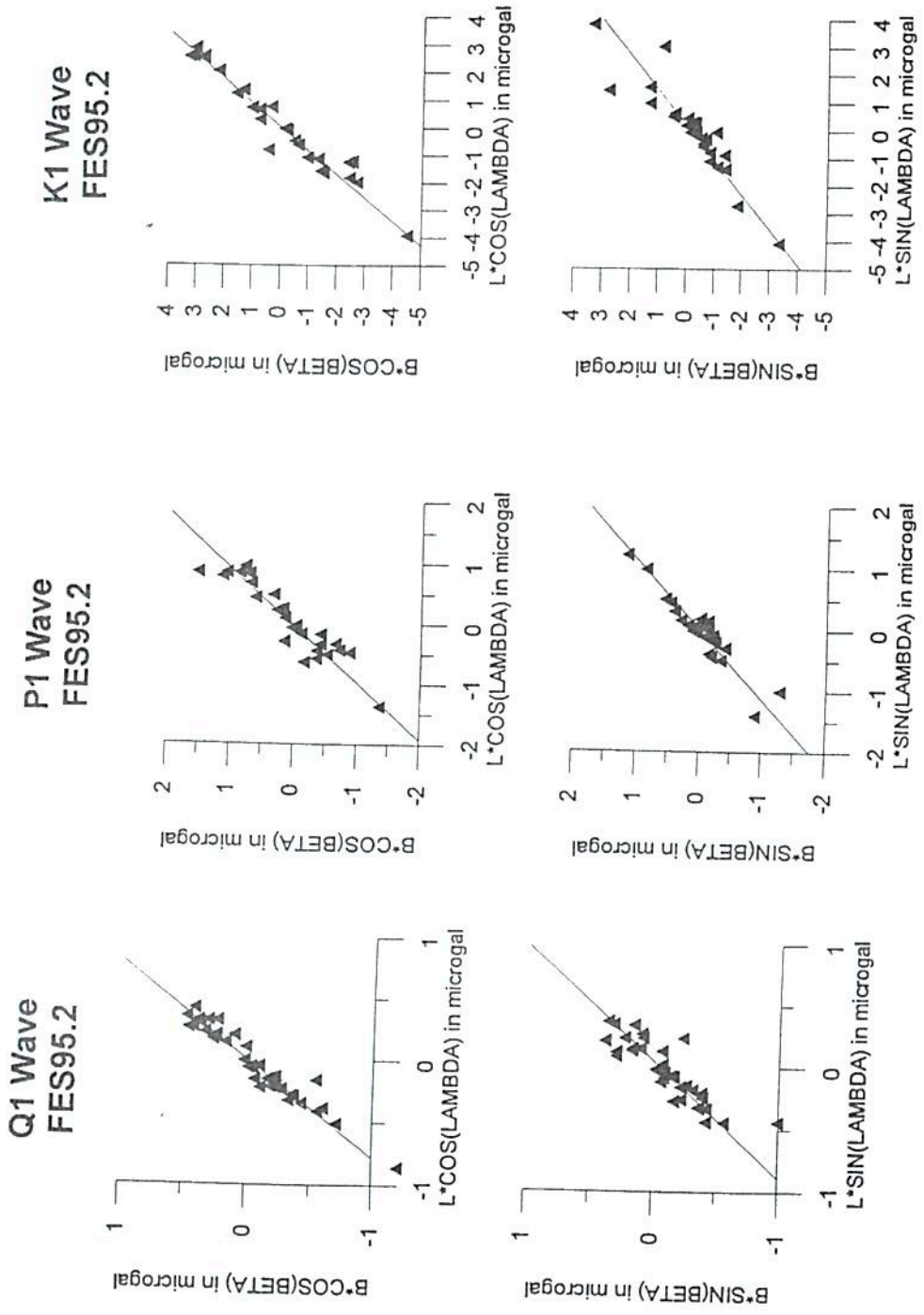

Table 1 — Gravity Tides - M2 Wave

δ, α Tidal parameters obtained with independently calibrated gravimeters after Oceanic Loading Correction

EUROPE

	Station	Ins.	N	Oceanic Models: SCHW80 δ	SCHW80 α	CSR3.0 δ	CSR3.0 α	FES95.2 δ	FES95.2 α	FES95.2b δ	FES95.2b α
0200	Bruxelles	Supra3	121920	1.1539	0.04°	1.1682	-0.18°	1.1586	0.04°	1.1591	-0.18°
0243	Membach	Supra21	8264	1.1565	-0.02°	1.1653	-0.14°	1.1607	0.01°	1.1614	-0.03°
0243	Membach	Absolu FG5	1139	1.1547	-0.20°	1.1637	-0.33°	1.1598	-0.17°	1.1589	-0.15°
0243	Membach	Scintrex	3840	1.1560	0.09°	1.1648	-0.04°	1.1602	0.12°	1.1610	0.14°
0306	Strasbourg	Supra 5	74170	1.1582	-0.04°	1.1618	-0.03°	1.1597	-0.08°	1.1591	-0.02°
0401	Valle d.L.C.	ET 15	5184	1.1593	0.28°	1.1643	-0.07°	1.1592	0.25°	1.1596	0.15°
0402	Madrid	LCR 665	6240	1.1632	0.04°	1.1674	-0.28°	1.1639	0.00°	1.1631	-0.10°
0515	Brasimone	Supra 15	6144	1.1598	-0.29°	1.1594	0.01°	1.1592	0.00°	1.1583	-0.06°
0610	Chur	ET 13	2496	1.1590	-0.16°	1.1607	-0.07°	1.1595	0.00°	1.1590	-0.07°
0615	Zurich	ET 13	5136	1.1592	-0.22°	1.1613	-0.16°	1.1598	-0.05°	1.1587	-0.14°
0701	Bonn	LCR 298	3696	1.1559	0.00°	1.1637	-0.11°	1.1600	0.05°	1.1596	-0.07°
0716	Schiltach	ET 19	9744	1.1586	-0.12°	1.1617	-0.08°	1.1601	0.02°	1.1590	-0.07°
0716	Schiltach	LCR 249	2880	1.1577	-0.08°	1.1609	-0.04°	1.1592	0.06°	1.1581	-0.03°
0734	Bad Homburg	ET 15	4464	1.1569	-0.03°	1.1626	-0.07°	1.1601	0.04°	1.1593	-0.04°
0765	Potsdam	A 222	186816	1.1567	-0.09°	1.1672	-0.14°	1.1632	-0.12°	1.1625	-0.11°
0765	Potsdam	Supra 18	26640	1.1571	-0.04°	1.1635	-0.07°	1.1615	0.01°	1.1608	-0.06°
0765	Potsdam	ET 16	5808	1.1556	-0.02°	1.1621	-0.05°	1.1601	0.03°	1.1594	-0.04°
0930	Pecny	A 228	87312	1.1589	-0.25°	1.1627	-0.24°	1.1614	-0.17°	1.1605	-0.23°
0950	Budapest	A 228	8160	1.1602	-0.11°	1.1628	-0.13°	1.1621	-0.07°	1.1613	-0.11°
1010	Sofia	A 220	7728	1.1573	-0.10°	1.1583	-0.22°	1.1582	-0.15°	1.1575	-0.18°
Mean		20 series		1.1577	-0.07°	1.1636	-0.12°	1.1607	0.00°	1.1598	-0.07°
			±	0.0004	0.03°	0.0007	0.03°	0.0003	0.03°	0.0003	0.03°

DB92 Europe, 84 stations: Melchior 1994(Schw80 Model) 1.1597 -0.09°
± 0.0007 0.04°

DB92 World, 215 stations: Melchior 1994(Schw80 Model) 1.1602 -0.09°
± 0.0005 0.03°

Inelastic non-hydrostatic model Dehant-Defraigne-Wahr 1997 1.16257

Correction for inertia not applied
Phase : minus is a lag
Ins : gravimeter
A : Askania GS15
ET : LaCoste Romberg Earth Tide
LCR : LaCoste Romberg Model G
Supra : Supraconducting Gravimeter
Absolu: Absolute Gravimeter
N : number of hourly readings

Table 2 — Gravity Tides - M2 Wave

δ, α Tidal parameters obtained with 10 gravimeters calibrated according to DB 92 system after Oceanic Loading Correction

SOUTH AMERICA CONTINENT

	Station	Ins.	N	Oceanic Models: SCHW80 δ	SCHW80 α	CSR3.0 δ	CSR3.0 α	FES95.2 δ	FES95.2 α	FES95.2b δ	FES95.2b α
6911	Morne/Cadets	G 783	3696	1.1567	-0.09°	1.1646	-0.27°	1.1652	-0.10°	1.1693	0.09°
6975	St Augustine	L 402	2736	1.1635	-0.15°	1.1676	-0.58°	1.1673	-0.55°	1.1731	-0.28°
7201	Caracas	L 402	3648	1.1547	-0.46°	1.1582	-0.66°	1.1581	-0.49°	1.1620	-0.55°
7250	Bogota	L 402	2640	1.1662	-0.51°	1.1711	-0.62°	1.1709	-0.45°	1.1734	-0.41°
7251	Cartagena	G 84	3168	1.1517	-0.64°	1.1560	-0.84°	1.1499	-0.64°	1.1588	-0.78°
7253	Cucuta	G 84	3744	1.1459	-0.42°	1.1499	-0.54°	1.1493	-0.42°	1.1524	-0.48°
7254	Cali	L 402	1344	1.1624	-0.99°	1.1700	-1.17°	1.1696	-0.45°	1.1725	-0.35°
7281	Kourou	G 783	4080	1.1644	-0.46°	1.1776	-0.26°	1.1766	-0.26°	1.1779	-0.24°
7303	Sao Paulo	L 913	7776	1.1609	0.02°	1.1588	-0.57°	1.1538	-0.35°	1.1556	-0.53°
7305	Curitiba	ET 10	4656	1.1622	0.25°	1.1594	-0.21°	1.1542	-0.18°	1.1564	-0.29°
7307	Campo Grande	L 003	1728	1.1627	-0.10°	1.1633	-0.32°	1.1623	-0.36°	1.1636	-0.39°
7309	Cuiaba	G 783	2640	1.1549	0.31°	1.1562	0.14°	1.1557	0.11°	1.1574	0.11°
7310	Goiania	G 783	3600	1.1540	0.31°	1.1553	0.10°	1.1548	0.08°	1.1543	0.04°
7311	Caico	L 008	4656	1.1590	0.30°	1.1656	-0.10°	1.1661	-0.12°	1.1703	-0.20°
7312	P.Prudente	L 487	4080	1.1618	-0.19°	1.1611	-0.46°	1.1598	-0.48°	1.1608	-0.55°
7314	Vassouras	G 783	4560	1.1722	-0.05°	1.1692	-0.47°	1.1654	-0.37°	1.1658	-0.50°
7315	Manaus	L 003	3456	1.1577	-0.85°	1.1611	-0.94°	1.1613	-0.94°	1.1632	-0.91°
7317	Salvador	L 008	3456	1.1559	0.36°	1.1588	-0.87°	1.1631	0.10°	1.1614	-0.24°
7319	Valhinos	L 913	4320	1.1635	0.03°	1.1631	0.15°	1.1608	0.14°	1.1622	0.05°
7400	Arequipa	L 402	4464	1.1580	0.17°	1.1580	0.07°	1.1607	-0.17°	1.1646	0.04°
7409	Nania	G 84	4272	1.1609	0.12°	1.1531	-0.34°	1.1658	-0.18°	1.1690	0.11°
7410	Chiclayo	L 402	2544	1.1548	0.25°	1.1582	-0.51°	1.1618	-0.09°	1.1645	0.31°
7411	Iquitos	G 84	4320	1.1512	0.08°	1.1543	-0.07°	1.1544	-0.01°	1.1563	0.07°
7412	Nazca	G 84	3696	1.1571	-0.28°	1.1586	-0.57°	1.1598	-0.63°	1.1644	-0.38°
7450	Quito	L 402	3264	1.1531	-0.35°	1.1589	-0.56°	1.1593	-0.24°	1.1618	-0.12°
7451	Guayaquil	G 84	2880	1.1615	-0.78°	1.1680	(-1.32)°	1.1677	-0.83°	1.1710	-0.64°
7500	La Paz	L 402	4176	1.1562	-0.10°	1.1578	-0.31°	1.1585	-0.36°	1.1612	-0.25°
7505	Santa Cruz	G 84	2688	1.1583	-0.17°	1.1600	-0.36°	1.1597	-0.41°	1.1618	-0.36°
7810	Tandil	G 765	3840	1.1598	0.21°	1.1545	-0.10°	1.1534	-0.65°	1.1520	-0.16°
7812	Cordoba	G 765	1296	1.1646	0.05°	1.1652	-0.25°	1.1643	-0.41°	1.1660	-0.32°
7813	Corrientes	G 765	1776	1.1713	-0.05°	1.1703	0.18°	1.1690	-0.43°	1.1706	-0.43°
7814	Zonda	L 906	2976	1.1463	0.48°	1.1477	0.18°	1.1470	-0.03°	1.1496	0.14°
7815	San Lorenzo	G 765	3360	1.1583	-0.11°	1.1595	-0.35°	1.1592	-0.45°	1.1617	-0.37°
7895	Tacuarembo	L 906	4368	1.1540	0.03°	1.1516	-0.39°	1.1486	-0.55°	1.1506	-0.55°
Mean	34 stations			1.1588	-0.11°	1.1607	-0.38°	1.1603	-0.33°	1.1628	-0.27°
			±	0.0010	0.06°	0.0012	0.07°	0.0012	0.05°	0.0012	0.05°

DB92 Latin America, 46 stations: Melchior 1994(Schw80 Model) 1.1603 -0.04°
± 0.0012 ±0.07°

DB92 World, 215 stations: Melchior 1994(Schw80 Model) 1.1602 -0.09°
± 0.0005 0.03°

Inelastic non-hydrostatic model : Dehant-Defraigne-Wahr 1997 1.16257

Correction for inertia not applied
Phase: minus is a lag
Ins : gravimeter G: Geodynamics
L: LaCoste Romberg Model G
N : number of hourly readings

Table 3 — Gravity Tides - O1 Wave

δ, α Tidal parameters obtained with independently calibrated gravimeters after Oceanic Loading Correction

EUROPE

	Station	Ins.	N	Oceanic Models: SCHW80 δ	SCHW80 α	CRS3.0 δ	CRS3.0 α	FES95.2 δ	FES95.2 α
0200	Bruxelles	Supra 3	121920	1.1572	0.00°	1.1567	-0.06°	1.1579	-0.02°
0243	Membach	Supra 21	8264	1.1548	0.00°	1.1543	-0.05°	1.1553	-0.02°
0243	Membach	Absolu FG5	1139	1.1576	-0.03°	1.1571	-0.08°	1.1581	-0.05°
0243	Membach	Scintrex	3840	1.1535	0.02°	1.1531	-0.03°	1.1541	0.00°
0306	Strasbourg	Supra 5	74170	1.1529	0.06°	1.1526	-0.01°	1.1532	0.02°
0401	Valle d.L.C.	ET 15	5184	1.1508	0.08°	1.1506	0.01°	1.1507	0.04°
0402	Madrid	LCR 665	6240	1.1554	-0.10°	1.1551	-0.17°	1.1552	-0.14°
0515	Brasimone	Supra 15	6144	1.1509	0.14°	1.1503	-0.03°	1.1511	0.00°
0610	Chur	ET 13	2496	1.1524	0.00°	1.1522	-0.09°	1.1524	0.00°
0615	Zürich	ET 13	5136	1.1516	-0.01°	1.1513	-0.09°	1.1517	-0.01°
0701	Bonn	LCR 298	3696	1.1561	-0.12°	1.1557	-0.17°	1.1566	-0.15°
0716	Schiltach	ET 19	9744	1.1522	0.02°	1.1519	-0.04°	1.1525	-0.02°
0716	Schiltach	LCR 249	2880	1.1519	-0.02°	1.1516	-0.08°	1.1522	-0.06°
0734	Bad Homburg	ET 15	4464	1.1501	-0.03°	1.1497	-0.08°	1.1505	-0.06°
0765	Potsdam	A 222	186816	1.1541	-0.02°	1.1535	-0.05°	1.1545	-0.04°
0765	Potsdam	Supra 18	26640	1.1542	0.03°	1.1537	-0.09°	1.1547	0.01°
0765	Potsdam	ET 16	5808	1.1520	0.06°	1.1514	0.03°	1.1524	0.04°
0930	Pecny	A 228	87312	1.1515	-0.09°	1.1512	-0.14°	1.1519	-0.12°
0950	Budapest	A 228	8160	1.1540	-0.03°	1.1530	-0.08°	1.1544	-0.06°
1010	Sofia	A 220	7728	1.1544	-0.10°	1.1554	-0.22°	1.1546	-0.18°
Mean	20 series			1.1534	-0.01°	1.1531	-0.07°	1.1538	-0.04°
			±	0.0005	0.01°	0.0005	0.01°	0.0005	0.01°

DB92 Europe, 81 stations: Melchior 1994(Schw80 Model) 1.1537 -0.10°
± 0.0010 ±0.04°

DB92 World, 188 stations: Melchior 1994(Schw80 Model) 1.1550 -0.22°
± 0.0008 ±0.04°

Inelastic non hydrostatic model:
Dehant-Defraigne-Wahr 1997 1.15382

Correction for inertia not applied
Phase : minus is a lag
Ins : gravimeter A : Askania GS15
ET : LaCoste Romberg Earth Tide
LCR : LaCoste Romberg Model G
Supra : Superconducting Gravimeter
Absolu: Absolute Gravimeter
N : number of hourly readings

Table 4 a — Gravity Tides - O1, P1 and K1 Diurnal Waves

δ, α Tidal parameters obtained after Oceanic Loading Correction with Schwiderski models and Residues B,L,X

Station	Ins.	N	O1	P1	K1	O1		P1		K1		E(αP1)
0200/a Bruxelles	*Supra 3	5128	1.1574	1.1514	1.1379	0.04	109	0.06	49	0.33	40	0.01
0200/b			-0.01	-0.08	0.00	0.13	162	0.07	80	0.23	66	
0200/c						0.11	-2	0.04	-38	0.16	1	
0243/a Membach	*Supra 21	345	1.1556	1.1505	1.1364	0.07	143	0.10	44	0.38	36	0.02
0243/b			0.00	-0.02	0.04	0.14	164	0.06	75	0.20	62	
0243/c						0.08	1	0.06	7	0.21	11	
0243/a Membach	Scintrex	168	1.1536	1.1474	1.1330	0.13	155	0.06	77	0.36	71	0.13
0243/b			0.02	-0.03	0.19	0.14	164	0.06	75	0.20	62	
0243/c						0.03	34	0.01	-	0.17	82	
0257/a Walferdange	A 233	4400	1.1566	1.1499	1.1376	0.07	-156	0.07	89	0.28	32	0.08
0257/b			-0.09	0.02	-0.04	0.15	170	0.07	76	0.21	63	
0257/c						0.10	-32	0.00	-	0.14	-15	
0306/a Strasbourg	*Supra 5	1254	1.1529	1.1481	1.1345	0.18	-12	0.07	97	0.16	57	0.02
0306/b			0.06	0.04	-0.04	0.15	172	0.06	78	0.18	65	
0306/c						0.33	-10	0.02	154	0.03	-76	
0401/a Valle d L.C.	ET 15	270	1.1508	1.1531	1.1378	0.56	-156	0.04	101	0.36	82	0.14
0401/b			0.08	-0.26	0.02	0.28	-139	0.12	111	0.34	101	
0401/c						0.33	-105	0.08	-65	0.11	10	
0402/a Madrid	LCR 665	270	1.1554	1.1474	1.1406	0.30	-129	0.16	121	0.38	66	0.12
0402/b			-0.10	0.11	0.04	0.26	-139	0.11	111	0.32	101	
0402/c						0.06	-85	0.05	143	0.22	9	
0515/a Brasimone	Supra 15	1220	1.1525	1.1499	1.1330	0.19	167	0.05	96	0.24	105	0.05
0515/b			0.06	0.02	0.13	0.13	178	0.05	99	0.12	88	
0515/c						0.06	143	0.03	0	0.14	121	
0615/a Zürich	ET 15	214	1.1516	1.1346	1.1337	0.23	178	0.24	156	0.37	91	0.10
0615/b			-0.01	0.16	0.25	0.15	175	0.06	82	0.16	70	
0615/c						0.08	-176	0.23	170	0.23	105	
0698/a Wien	LCR 9	149	1.1587	1.1447	1.1381	0.12	90	0.10	140	0.18	33	0.18
0698/b			0.13	0.09	0.01	0.13	160	0.03	88	0.09	75	
0698/c						0.16	41	0.08	157	0.13	5	

Table 4b

0709/a Hannover	5 instr.		1.1525	1.1455	1.1351	0.06	148	0.08	125	0.06	-7	0.13
0709/b			0.05	0.24	-0.01	0.14	155	0.05	66	0.17	51	
0709/c						0.08	-20	0.07	161	0.15	-108	
0716/a Schiltach	*ET 19	286	1.1525	1.1464	1.1330	0.21	172	0.09	115	0.25	93	0.05
0716/b			0.01	0.09	0.11	0.15	172	0.06	79	0.17	66	
0716/c						0.06	173	0.05	156	0.13	131	
0734/a Bad Homburg	*Supra 1	1004	1.1494	1.1444	1.1308	0.30	-170	0.07	167	0.13	138	0.01
0734/b			-0.15	-0.14	-0.07	0.14	164	0.06	73	0.17	59	
0734/c						0.18	-150	0.09	-152	0.19	-162	
0765/a Potsdam	*Supra 18		1.1542	1.1493	1.1351	0.16	133	0.04	60	0.27	58	0.02
0765/b			0.03	-0.11	0.09	0.14	153	0.05	62	0.14	47	
0765/c						0.05	75	0.01	-	0.14	69	
0930/a Pecny	A 131	1768	1.1539	1.1500	1.1350	0.17	146	0.06	85	0.31	81	0.17
0930/b			0.07	0.07	0.25	0.14	158	0.04	76	0.11	61	
0930/c						0.05	106	0.02	106	0.21	91	
2005/a Ankara	G 783	350	1.1638	1.1450	1.1421	0.20	-52	0.15	-163	0.12	47	0.17
2005/b			-0.39	-0.28	-0.02	0.16	151	0.07	150	0.22	151	
2005/c						0.28	-18	0.11	-136	0.29	18	
2605/a Lanzhou	2 instr.		1.1552	1.1537	1.1392	0.32	-20	0.13	15	0.38	-11	0.17
2605/b			-0.22	0.19	-0.12	0.30	4	0.07	-7	0.23	2	
2605/c						0.13	-89	0.07	38	0.17	-30	
2606/a Urumqi	G 84	186	1.1601	1.1412	1.1420	0.25	11	0.17	-136	0.31	-13	0.30
2606/b			-0.16	-0.62	-0.30	0.17	59	0.06	87	0.19	87	
2606/c						0.19	-31	0.22	-125	0.39	-41	
2607/a Wuhan	2 instr.		1.1549	1.1467	1.1376	0.72	-26	0.32	-36	0.80	-43	0.18
2607/b			-0.22	-0.28	-0.28	0.65	-18	0.20	-39	0.63	-32	
2607/c						0.12	-76	0.13	-31	0.22	-78	
2612/a Shanghai	G 783	331	1.1531	1.1527	1.1409	1.05	-17	0.43	-24	1.83	-36	0.28
2612/b			-0.24	0.21	-0.61	1.21	-8	0.43	-32	1.43	-25	
2612/c						0.23	-146	0.06	62	0.51	-70	
2849/a Esashi	LCR 457	365	1.1603	1.1502	1.1433	2.06	15	0.78	-2	2.94	-3	0.12
2849/b			-0.52	-0.34	-0.45	2.16	23	0.79	5	2.63	5	
2849/c						0.32	-90	0.11	-123	0.49	-49	
3090/a Cueva/los V.	2 instr.		1.1565	1.1465	1.1356	0.88	-92	0.24	175	0.58	159	0.19
3090/b			-0.71	-0.28	-0.07	0.50	-95	0.20	157	0.57	154	
3090/c						0.38	-88	0.08	-135	0.05	-120	

Table 4c

4209/a Alice Springs*G 84	352	1.1611	1.1525	1.1435	0.58	-121	0.27	-118	0.74	-133	0.17
4209/b		0.13	0.50	0.11	0.52	-122	0.18	-133	0.55	-121	
4209/c					0.06	-110	0.11	-78	0.23	-163	
6024/a Pinon Flat Supra 1	554	1.1611	1.1570	1.1474	1.81	84	0.93	69	3.02	65	0.03
6024/b		-0.04	-0.13	-0.20	1.82	89	0.93	75	3.00	74	
6024/c					0.16	-7	0.10	-18	0.47	-18	
6803/a Ottawa ET 12	2841	1.1632	1.1565	1.1419	0.55	30	0.21	75	0.76	26	0.15
6803/b		-0.10	-0.29	-0.22	0.40	57	0.20	54	0.65	53	
6803/c					0.16	-7	0.10	-18	0.47	-33	
7305/a Curitiba ET 10	194	1.1544	1.1429	1.1340	0.71	128	0.06	39	0.27	98	0.11
7305/b		-0.28	0.12	-0.07	0.64	138	0.08	126	0.25	119	
7305/c					0.13	75	0.10	-15	0.10	30	
9904/a Kerguelen A 206	390	1.1618	1.1441	1.1332	1.09	-142	0.39	-83	1.62	-124	0.40
9904/b		-0.33	0.10	0.38	1.19	-133	0.37	-106	1.05	-108	
9904/c					0.21	103	0.15	-11	0.68	-30	

* Atmospheric correction applied

A : Askania GS 15
ET : LaCoste Romberg Earth Tide
G : Geodynamics
LCR : LaCoste Romberg Model G
SUPRA : Superconducting gravimeter

Correction for inertia not applied
Phases : minus is a lag
N is here the number of days allowing the P1, K1 separation

Residues B according to Dehant-Defraigne-Wahr inelastic model 1997

Table 5 Gravity Tides - Q1 Wave

δ, α Tidal parameters obtained after Oceanic Loading Correction with Schwiderski Model

EUROPE

L(Q1) < 0.05 μgal except stations 0401/0402 where L(Q1) = 0.10μgal

	Station	Ins.	N	δ	α
0200	Bruxelles	Supra 3	121930	1.1537 ± 0.0004	-0.01° ± 0.02°
0243	Membach	Supra 21	8264	1.1519 ± 0.0004	-0.05° ± 0.03°
0257	Walferdange	A 233	90384	1.1552 ± 0.0018	-0.16° ± 0.09°
0306	Strasbourg	Supra 5	74170	1.1519 ± 0.0013	-0.00° ± 0.07°
0401	Valle d.L.C.	ET 15	5184	1.1474 ± 0.0086	-0.22° ± 0.42°
0402	Madrid	L 665	6240	1.1632 ± 0.0054	0.07° ± 0.27°
0515	Brasimone	Supra 15	6144	1.1526 ± 0.0012	-0.35° ± 0.06°
0610	Chur	ET 13	2496	1.1449 ± 0.0055	-0.03° ± 0.27°
0615	Zürich	ET 13	5136	1.1540 ± 0.0044	-0.14° ± 0.27°
0698	Wien	LCR 9	4656	1.1570 ± 0.0010	-0.21° ± 0.48°
0709	Hannover	5 LCR	12970	1.1515 ± 0.0009	0.13° ± 0.14°
0716	Schiltach	ET 19	9744	1.1497 ± 0.0019	0.08° ± 0.09°
0734	Bad Homburg	ET 15	4464	1.1492 ± 0.0006	-0.09° ± 0.03°
0765	Potsdam	Supra 18	26640	1.1528 ± 0.0007	0.03° ± 0.03°
0765	Potsdam	A 222	186816	1.1522 ± 0.0013	-0.06° ± 0.06°
0765	Potsdam	ET 16	5808	1.1547 ± 0.0055	0.17° ± 0.27°
0930	Pecny	A 228	87312	1.1493 ± 0.0011	-0.14° ± 0.06°
Mean		17 series		1.1524 ± 0.0006	-0.06° ± 0.03°

Inelastic non-hydrostatic model
Dehant-Defraigne-Wahr 1997 1.1538

Correction for inertia not applied
Phase : minus is a lag
Ins : gravimeter
A : Askania GS15
ET : LaCoste Romberg Earth Tide
LCR : LaCoste Romberg Model G
SUPRA: Superconducting Gravimeter
N : number of hourly readings

Table 6 Regression parameters between the tidal Residues B and gravity loading effects L for 223 tidal stations and for the Q1 wave (B = a+b L). a and mean-square errors are in microgal.

Parameters	SCHW80	CSR3.0	FES95.2	ORINA0
In-phase				
a	-0.029 ± 0.010	-0.029 ± 0.010	-0.006 ± 0.010	-0.019 ± 0.010
b	1.260 ± 0.015	1.133 ± 0.067	1.268 ± 0.075	1.270 ± 0.075
Correlation coefficient	0.747	0.751	0.752	0.751
Mean-square error	0.149	0.148	0.148	0.148
Out-of-phase				
a	-0.017 ± 0.009	-0.012 ± 0.009	-0.027 ± 0.008	-0.007 ± 0.008
b	1.311 ± 0.077	1.028 ± 0.059	1.235 ± 0.072	1.097 ± 0.060
Correlation coefficient	0.754	0.758	0.756	0.776
Mean-square error	0.131	0.125	0.129	0.122

Table 7 Gravity Tides - Q1 Wave

33 Stations where L (Q1) ≥ 0.2 μgal

	Station	Latit.	A	δ	α	B	β	SCHW80		CSR3.0		FES95.2	
821	Faeroe	62 4	5.49	1.1608	-0.45	0.29	-133	0.29	-144	0.31	-166	0.27	-144
2555	Kota Kinabalu	5 57	1.61	1.1471	-5.56	0.57	-80	0.44	-75	0.64	-69	0.49	-65
2600	Guangzhou	25 6	5.15	1.1586	-1.21	0.33	-59	0.24	-42	0.30	-52	0.21	-45
2601	Hong Kong	22 18	5.10	1.1581	-1.19	0.46	-56	0.39	-49	0.48	-54	0.32	-50
2612	Shanghai	31 6	6.42	1.1771	-0.53	0.34	-12	0.24	-3	0.25	-2	0.23	5
2823	Kyoto	35 2	6.80	1.1571	-0.13	0.34	18	0.34	20	0.33	18	0.31	29
2849	Esashi	39 9	7.10	1.1585	-0.93	0.41	14	0.43	29	0.43	33	0.40	42
2875	Kanoya	31 25	6.54	1.1600	-1.32	0.44	-9	0.42	10	0.52	7	0.44	17
2877	Tokyo 34	35 43	6.84	1.1491	-3.53	0.40	-35	0.41	24	0.46	26	0.40	36
2877	Tokyo 447	35 43	6.77	1.1352	-0.76	0.28	18	0.41	24	0.46	26	0.40	36
2877	Tokyo 783	35 43	6.92	1.1620	0.52	0.47	29	0.41	24	0.46	26	0.40	36
2897	Memambetsu	43 54	7.38	1.1707	1.17	0.63	35	0.47	28	0.53	32	0.51	46
3019	Arta	11 32	2.55	1.1738	3.76	0.34	118	0.23	148	0.23	129	0.19	141
3020	Mogadiscio	2 1	0.44	1.2159	23.77	0.47	125	0.31	144	0.36	134	0.31	137
4010	Baguio	16 24	4.27	1.2226	1.14	0.50	-19	0.35	-42	0.93	-63	0.38	-46
4105	Banjar Baru	-3 20	0.89	1.2819	7.05	0.42	-91	0.32	-74	0.49	-75	0.35	-72
4110	Ujung Pandang	-5 40	1.66	1.2608	23.99	0.99	-91	0.39	-89	0.65	-85	0.44	-90
4115	Kupang	-10 11	2.54	1.1530	0.27	0.44	-105	0.43	-106	0.62	-100	0.49	-116
4210	Darwin	-12 51	3.31	1.2278	-2.10	0.34	-170	0.23	-130	0.38	-133	0.34	-160
4211	Mundaring	-31 59	6.75	1.2385	0.28	0.67	-149	0.34	-112	0.41	-117	0.36	-166
4220	Hobart	-42 55	7.43	1.1895	-1.63	0.65	153	0.39	166	0.44	166	0.42	168
6004	Uwekahuna	19 25	4.26	1.1790	-1.55	0.17	107	0.31	115	0.38	115	0.37	114
6024	Pinon Flat	33 36	6.31	1.1612	-0.33	0.32	95	0.36	99	0.37	96	0.35	100
6911	Morne/Cadets	14 44	3.66	1.1718	0.87	0.33	32	0.26	27	0.30	25	0.22	38
7314	Vassouras	-22 24	5.08	1.1846	-0.21	0.29	144	0.20	129	0.25	130	0.20	131
7810	Tandil	-37 19	7.02	1.1744	0.35	0.41	-167	0.30	-171	0.33	-167	0.29	-171
7817	Ushuaia	-54 49	7.21	1.2013	-0.13	0.77	-163	0.53	-154	0.63	-151	0.57	-153
7818	Com.Rivadavia	-45 50	7.49	1.2015	0.31	0.64	-166	0.37	-161	0.44	-161	0.39	-169
7819	Santa Rosa	-36 38	6.79	1.1570	0.45	0.23	-143	0.22	-157	0.24	-155	0.22	-161
9904	Kerguelen	-49 21	6.60	1.1676	1.46	0.41	-118	0.26	-127	0.34	-124	0.25	-124
9910	C.Ferraz	-62 5	6.91	1.2472	0.67	1.28	-163	0.82	-158	0.99	-159	0.92	-159
9941	Asuka	-71 32	4.50	1.1839	-0.36	0.38	-168	0.28	-158	0.32	-159	0.29	-163
9960	Syowa	-69 0	5.05	1.1799	1.74	0.54	-145	0.39	-154	0.47	-152	0.39	-152

Superconducting Gravimeters

201	Bruxelles	50 48	6.71	1.1538	-0.01	0.03	-117	0.03	-126	0.04	258	0.06	206
306	Strasbourg	48 37	6.75	1.1519	0.00	0.12	-145	0.04	-127	0.05	238	0.05	215
765	Potsdam	52 23	6.60	1.1528	0.03	0.04	-152	0.04	-147	0.03	228	0.05	200

A observed amplitude in μgal
δ, α corrected Schwiderski model
Correction for inertia not applied
Phases : minus is a lag
Earth Model δ(Q1) = 1.1538

Table 8 Gravity Tides - P1 Wave

27 Stations where L (P1) ≥ 0.2 μgal and N > 180 days

	Station	Latit.	A	δ	α	B	β	SCHW80		CSR3.0		FES95.2	
2600	Guangzhou	23 06	12.00	1.1535	0.33	0.33	-90	0.40	-92	0.53	-95	0.48	-92
2612	Shanghai	31 06	15.09	1.1527	0.21	0.43	-24	0.43	-32	0.51	-35	0.65	-41
2823	Kyoto 783	35 02	16.37	1.1578	-0.47	0.77	-15	0.64	-7	0.71	-7	0.69	-7
2847	Mizusawa 402	39 08	17.46	1.1410	-2.59	1.19	4	0.75	5	0.81	6	0.80	6
2849	Esashi	39 09	17.05	1.1502	-0.34	0.78	-2	0.79	5	0.86	7	0.84	7
2877	Tokyo 34	35 43	16.88	1.1770	0.52	1.13	6	0.77	-2	0.94	0	0.86	0
2877	Tokyo 783	35 43	16.67	1.1616	0.27	0.92	3	0.77	-2	0.94	0	0.86	0
2877	Tokyo 447	35 43	17.32	1.2094	-0.40	1.57	-5	0.77	-2	0.94	0	0.86	0
2897	Memambetsu	43 54	17.54	1.1500	-0.75	0.85	-9	0.86	6	0.98	6	0.97	9
3019	Arta	11 31	6.03	1.1579	0.57	0.65	141	0.63	147	0.67	148	0.59	148
3020	Mogadiscio	2 01	1.16	(1.5616)	(0.90)	0.58	105	0.78	137	0.89	142	0.81	141
4105	Banjar Baru	-3 20	3.07	(1.4684)	(10.64)	1.54	-124	0.90	-115	1.25	-124	1.10	-115
4115	Kupang	-10 11	6.21	1.1182	-0.79	0.95	-111	1.09	-118	1.41	-116	1.52	-112
4209	Alice Springs	-23 43	12.37	1.1525	0.50	0.27	-118	0.18	-133	0.21	-130	0.25	-128
4220	Hobart	-42 55	17.34	1.1775	-0.07	0.90	148	0.59	129	0.73	126	0.62	133
6004	Uwekahuna	19 25	10.67	1.1975	0.70	1.18	84	1.06	103	1.48	105	1.26	103
6024	Pinon Flat	33 36	15.67	1.1561	-0.13	0.92	69	0.93	75	1.13	79	1.02	77
6340	Pittsburgh	40 25	16.63	1.1578	0.52	0.38	55	0.20	55	0.21	61	0.20	58
6911	Morne/Cadets	14 44	8.82	1.1822	1.21	0.67	17	0.43	3	0.50	11	0.45	11
7201	Caracas	10 30	6.22	1.1659	-0.64	0.26	-9	0.19	7	0.27	6	0.25	15
7281	Kourou	5 10	3.18	1.1442	1.26	0.20	-17	0.25	-30	0.28	-18	0.28	-20
7408	Arequipa	-16 28	9.71	1.1964	1.00	0.78	-149	0.40	-143	0.49	-140	0.43	-139
7409	Nana	-11 59	7.18	1.1699	-1.55	0.44	-163	0.45	-136	0.71	-131	0.50	-131
7450	Quito	-0.13	0.63	(3.5747)	(15.71)	0.52	-152	0.22	-147	0.24	-142	0.22	-138
7818	Com.Rivadavia	-45 50	17.02	1.1525	0.32	0.40	175	0.38	162	0.40	168	0.45	166
9904	Kerguelen	-49 21	15.56	1.1432	0.10	0.39	-83	0.37	-106	0.32	-99	0.29	-101
9910	Com.Ferraz	-62 05	15.16	1.1643	0.50	1.41	180	1.23	174	1.40	169	1.39	172

A : observed amplitude in μgal
δ,α : corrected Schwiderski model
Correction for inertia not applied
Phases : minus is lag
Earth Model δ(P1) = 1.1487

Table 9 Gravity Tides - K1 Wave

27 Stations where L (P1) ≥ 0.2 μgal and N > 180 days

	Station	Latit.	A	δ	α	B	β	SCHW80		CSR3.0		FES95.2	
2600	Guangzhou	23 06	35.68	1.1329	-0.32	1.39	-95	1.18	-90	1.59	-97	1.38	-93
2612	Shanghai	31 06	45.33	1.1410	-0.61	1.83	-36	1.43	-25	1.50	-36	1.88	-44
2823	Kyoto 783	35 02	48.98	1.1430	-0.51	2.47	-15	2.11	-6	2.11	-8	2.06	-8
2847	Mizusawa 305	39.08	51.44	1.1410	-0.80	2.94	-9	2.66	5	2.54	5	2.50	6
2849	Esashi	39 09	51.48	1.1434	-0.45	2.94	-3	2.63	5	2.54	6	2.50	6
2877	Tokyo 34	35 43	50.43	1.1579	-0.28	3.45	-5	2.54	-2	2.80	-2	2.56	-1
2877	Tokyo 783	35 43	49.89	1.1444	-0.05	2.90	-2	2.54	-2	2.80	-2	2.56	-1
2877	Tokyo 447	35 43	50.28	1.1541	-1.17	3.44	-18	2.54	-2	2.80	-2	2.56	-1
2897	Memambetsu	43 54	52.78	1.1467	-0.23	3.24	0	2.77	5	2.91	5	2.90	9
3019	Arta	11 31	18.09	1.1563	0.56	1.97	136	2.06	146	2.14	147	1.84	148
3020	Mogadiscio	2 01	1.57	(0.8255)	-6.02	3.00	153	2.35	137	2.80	142	2.52	142
4105	Banjar Baru	-3 20	7.47	(1.2031)	-1.92	2.35	-129	2.62	-117	3.75	-127	3.17	-121
4115	Kupang	-10 11	20.02	1.2119	0.95	4.15	-127	3.29	-114	4.35	-118	4.47	-114
4209	Alice Springs	-23 43	37.01	1.1436	0.11	0.74	-133	0.55	-121	0.62	-131	0.72	-130
4220	Hobart	-42 55	52.01	1.1746	-1.78	3.77	131	1.54	126	2.21	124	1.90	131
6004	Uwekahuna	19 25	31.81	1.1833	-0.13	3.43	81	3.55	102	4.54	104	3.89	102
6024	Pinon Flat	33 36	47.07	1.1475	-0.20	3.02	65	3.00	74	3.44	77	3.10	76
6340	Pittsburgh	40 25	49.87	1.1482	-0.02	1.06	29	0.66	54	0.64	60	0.60	59
6911	Morne/Cadets	14 44	26.05	1.1542	-0.63	1.67	-6	1.40	5	1.50	12	1.27	14
7201	Caracas	10 30	18.59	1.1505	-0.20	0.75	3	0.62	11	0.81	12	0.69	18
7281	Kourou	5 10	9.99	1.1730	-0.78	0.94	-31	0.88	-24	0.80	-18	0.77	-20
7408	Arequipa	-16 28	27.92	1.1339	0.19	1.25	-140	1.26	-145	1.50	-143	1.33	-144
7409	Nana	-11 59	21.48	1.1524	-0.52	1.54	-149	1.51	-137	2.20	-135	1.58	-136
7450	Quito	-0.13	1.21	1.1198	(28.72)	0.91	-136	0.74	-147	0.79	-146	0.76	-144
7818	Com.Rivadavia	-45 50	52.19	1.1696	0.76	2.66	-174	1.22	-199	1.17	-189	1.26	-193
9904	Kerguelen	-49 21	49.79	1.1333	0.38	1.62	-124	1.05	-108	1.03	-92	0.87	-92
9910	Com.Ferraz	-62 05	45.67	1.1649	-0.07	4.68	174	3.57	173	4.10	169	3.98	171

A : observed amplitude in μgal
δ,α : corrected Schwiderski model
Correction for inertia not applied
Phases : minus is lag
Earth model δ(K1) = 1.1345

Influence of the Cavity Effect on Tidal Measurements

Brimich L.[1], Kohút I.[1], Kostecký P.[2]
[1]Geophysical Institute, Slovak Academy of Sciences, Dúbravská cesta 9, Bratislava
[2]Department of Geophysics, Faculty of Mathematics and Physics, Comenius University, Bratislava

Introduction

Tidal forces generate periodic, low-frequency loading of the Earth's interior. Measurements of tidal-induced strain and tilt are usually performed in underground facilities, mostly in order to minimize influence of environmental factors (e.g. air temperature changes). In the underground galleries the tidal measurements are affected by some local perturbations which have been clearly isolated and tentatively evaluated (*Melchior 1978*). These effects cause a distortion of the regional strain field by the change of geometry of the underground cavity (mine, cave, gallery) containing the tidal instruments. This change is called cavity effect. The distortion of the regional strain field produced by topography of the free surface in the vicinity of the observatory is known as a topographic effect and a distortion of the regional strain field caused by the geological inhomogeneities of the rocks surrounding the tidal observatory is the geologic effect. These effects are generated by tidal forces and alterate the phase and the amplitude of the tidal phenomena. The disorders due to local effects have the tidal periodicity (they are induced by the earth's tides). Considering this fact it is not possible to separate the influences of these effects from the tidal measurements by frequency analysis. If the cavity, where the earth's tide station is located, is deep enough with respect to the topographic features, then the topographic effects and cavity deformations do not interact and can be treated separately. This means that the underground station must be deep below the near-by topographic features. In (*Brimich and Brestenský 1992*) the local effects at the tidal station Vyhne were estimated using h-version of the finite element method. It was shown that in the depth 65 m